

Impact of HSDPA Transmit Power Allocation Schemes on the Performance of UMTS Networks

Andreas Mäder, Dirk Staehle, Rastin Pries and Markus Spahn
University of Würzburg, Institute of Computer Science, Department of Distributed Systems
Am Hubland, D-97074 Würzburg, Germany
{maeder, staehle, pries, spahn}@informatik.uni-wuerzburg.de

Abstract—In UMTS networks, the transmit power for the HSDPA can be a large fraction of the total transmit power of a NodeB. We investigate the impact of three HSDPA transmit power allocation schemes on the performance of a UMTS system with dedicated channel users and HSDPA users. The continuous HSDPA power allocation scheme avoids large steps of the transmit power in order to prevent irregularities in the downlink power control of dedicated channels. In contrast, the traffic-aware scheme switches the HSDPA power on only if data has to be transmitted. The power-ramping scheme combines the continuous and the traffic-aware scheme. The simulation model considers the complete interference situation in the network and uses a novel model to calculate HSDPA bandwidths. The results quantify the performance loss with the continuous scheme caused by additional interference, and show that the power-ramping scheme leads to results close to the traffic-aware scheme.

I. INTRODUCTION

The High Speed Downlink Packet Access (HSDPA) is either in deployment or in operation in most of the important mobile telecommunication markets. HSDPA is an enhancement of UMTS and has been introduced with Rel. 5 of the UMTS standard. One of the reasons which lead to the development of the HSDPA was the fact that “classical” dedicated channels (DCH) in Rel. 99 UMTS are inefficient for the transport of best effort traffic. DCH radio bearers follow a “circuit-switched” paradigm: each user gets a link with an agreed QoS level, i.e. bit rate, bit error rate, etc. Radio resource management (RRM) and the link layer takes care that this QoS level stays as constant as possible over time. Since best-effort traffic is typically bursty, this concept becomes inefficient since radio resources are occupied even in case of time periods without traffic, e.g. in case of web-browsing.

The concept of the HSDPA is to adapt the data rate to the instantaneous channel quality at the receiver by using channel quality information feedback. HSDPA uses a shared channel, the High Speed Downlink Shared Channel (HS-DSCH), which is used by all HSDPA users in a sector. The shared channel concept overcomes the drawbacks of dedicated channels regarding radio resource efficiency for bursty traffic, but a fixed QoS-level cannot be guaranteed anymore.

If the offered load for the HSDPA is not very high, periods without traffic alternate with periods with traffic. If we consider a “traffic-aware” transmit power scheme for the HS-DSCH, this means that the HS-DSCH is switched on and off possibly in a very fast pattern, since the minimum

scheduling time corresponds to the transport time interval (TTI) of 2 ms. This is a potential problem for the power control of DCH connections, since firstly, the power control step size is maximally ± 1 dB, but the maximum transmit power for the HS-DSCH is around 42.5 dBm (corresponds to approx. 18 W, if we assume 20 W maximum output power and 2 W pilot/common channels), and secondly, 2 ms TTI allows only for 3 power control commands (1 per slot).

Therefore, it may be beneficial to implement a more power control friendly HS-DSCH power allocation scheme, even if it may lead to additional interference. So, additionally to the traffic-aware scheme, we consider the continuous and the power-ramping scheme. In the continuous scheme we assume that the HS-DSCH is always ON, transmitting padding bits if no data is available. The power-ramping schemes avoids large interference steps by increasing and decreasing the HS-DSCH transmit power in small steps.

In this work we investigate the impact of such schemes on the amount of interference and the resulting impact on the performance of the HSDPA. However, we do not implement power control directly, since this would require the complete simulation of all power control commands in the whole network. Instead, we focus on the large-scale effects of the different schemes on the network-wide interference and the resulting impact on HSDPA bandwidth and blocking probabilities. For the numerical results, we use a flow-level event-discrete simulation with an analytic bandwidth model for the HSDPA, similar to that used in [1] and [2].

In the literature, power allocation schemes are mostly considered in the context of general radio resource management schemes. In [3] it is assumed that the HSDPA is always saturated with traffic, which then corresponds to a continuous transmit power scheme. In [4], it seems that a traffic-aware scheme has been implemented. However, to the best of our knowledge, an explicit comparison of different power allocation schemes can not be found in the literature.

In the next section we give a brief overview of relevant technical details. In Sec. III, we introduce the transmit power allocation schemes. In Sec. IV, the calculation of transmit powers is explained. Section V gives an overview of the HSDPA bandwidth model and the simulation model. Numerical results are shown in Sec. VI. Finally, in Sec. VII, we give a conclusion and point out some further topics of research.

II. SYSTEM DESCRIPTION

We consider a UMTS network where HSDPA and DCH connections share the same radio resources, namely transmit power and orthogonal codes. The core of the HSDPA is the HS-DSCH (high speed downlink shared channel), which uses up to 15 codes with spreading factor (SF) 16 in parallel. The HS-DSCH enables two types of multiplexing: Time multiplex by scheduling the subframes to different users, and code multiplex by assigning each user a non-overlapping subset of the available codes. The latter requires configuration of additional HS-SCCHs (High Speed Shared Control Channel). Throughout this work we assume that one HS-SCCH is present, hence consider time multiplex only.

In contrast to dedicated channels, where the transmit power is adapted to the propagation loss with fast power control and thus enabling a more or less constant bit rate, the HS-DSCH adapts the channel to the propagation loss with adaptive modulation and coding (AMC). The UE (user equipment) sends channel quality indicator (CQI) values to the NodeB. The CQI is a discretization of the received SIR at the UE and ranges from 0 (no transmission possible) to 30 (best quality). The scheduler in the NodeB then chooses a transport format combination (TFC) such that a pre-defined target BLER, which is often chosen as 10%, is fulfilled if possible. The TFC contains information about the modulation (QPSK or 16QAM), the number of used codes (from 1 to 15), and the coding rate resulting in a certain transport block size (TBS) that defines the information bits transmitted during a TTI. A number of tables in [5] define a unique mapping between CQI and TFC. This means that with an increasing CQI, the demand on code resources is also increasing. This leads to cases where a high CQI is reported at the NodeB, but the scheduler has to select a lower TBS due to lacking code resources.

Additionally to the transmit power, the OSVF-codes (orthogonal variable spreading factor codes) have to be considered due to their capacity-limiting properties [6]. Each cell¹ has a number of codes available, from which DCH connections normally require a fixed number of OSVF-codes per connection. The rest of the codes is available for the HS-DSCH.

III. TRANSMIT POWER ALLOCATION AND RADIO RESOURCE SHARING

In Fig. 1, the different HS-DSCH power allocation schemes are illustrated. The continuous scheme assumes that the power remaining from DCH connections is always used by the HS-DSCH, regardless whether data has to be transmitted or not. This means effectively, that the NodeBs always send with target power T^* . In contrast, the traffic-aware scheme switches the HS-DSCH off if no data is available for transmission. In this case, the transmit power is dominated by an ON-OFF pattern, where the length of the ON-phases depend on the number of active HSDPA users, the data volumes and the bit rate of the HSDPA users. In order to avoid large interference

¹Synonym to sector in this work

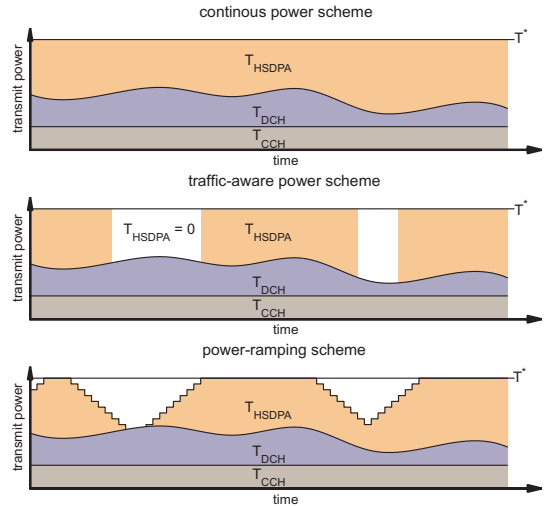


Fig. 1. Transmit power allocation schemes for the HS-DSCH

steps, the power-ramping scheme assumes that as soon as data is available for transmission for at least one user, the HS-DSCH transmit power is increased step-by-step until the target power is reached, i.e. a “power-ramp” is established. If no user is active anymore, HS-DSCH transmit power is decreased in the same way. Different possibilities exist for the implementation of power-ramping. We chose a linear scheme, i.e. the transmit power is increased and decreased in equal steps ΔT_{up} and ΔT_{down} . The time between two up/down steps is denoted with Δt_{step} and is equal for up and down ramping.

Throughout this work we consider adaptive radio resource sharing for the HSDPA, i.e. the HS-DSCH transmit power depends on the target transmit power T_x^* and the DCH transmit power $T_{x,d}$ in the following way:

$$T_{x,h} = \begin{cases} T_x^* - T_{x,c} - T_{x,d}, & \text{if not in ramping phase} \\ T_{x,r} & \text{else} \end{cases} \quad (1)$$

$$C_{x,h} = C_x - C_{x,c} - C_{x,d}, \quad (2)$$

where $T_{x,c}$ is used by common channels and the pilot. With power ramping and if in a ramping phase, the HS-DSCH transmit power is set to $T_{x,r}$ which is increased or decreased step-wise by ΔT_{up} and ΔT_{down} . The number of code units available for the HSDPA, $C_{x,h}$, is the maximum number of code units C_x minus the code resources required for DCH and the common channels. A code unit corresponds to an OSVF code with SF 512, which is the code with the highest spreading factor used in UMTS. All other codes can be expressed in terms of a multiple of this code unit, such that the number of code units occupied by a code is $c_s = \frac{512}{SF_s}$. The number of SF16 codes available for the HS-DSCH is then $N_{x,h} = \lfloor \frac{C_{x,h}}{32} \rfloor$.

IV. CALCULATION OF TRANSMIT POWERS

A UMTS network is defined as a set \mathcal{L} of NodeBs and with associated UEs, \mathcal{M}_x . A DCH user k corresponds to a RAB at NodeB $x \in \mathcal{L}$ that is defined by the code $C_{x,k}$, the information bit rate R_k , and a target bit-energy-to-noise ratio $(E_b/N_0) \varepsilon_k^*$. Furthermore, we define ν_k as the activity factor of the user which corresponds to the percentage of time the user is actually transferring data. Then, the transmit power requirement from NodeB x for a DCH user k is

$$T_{x,k} = \frac{\varepsilon_k^* \cdot R_k}{W} \cdot \left(\frac{W \cdot N_0 + I_k^{oth}}{d_{x,k}} + \alpha \cdot T_x \right), \quad (3)$$

where W denotes the system bandwidth of 3.84 Mcps, N_0 denotes the thermal noise spectral density of -174 dBm/Hz, α is the orthogonality factor which we assume to be constant like in [7], and $d_{x,k}$ is the average propagation gain from x to k . The other-cell interference I_k^{oth} is the total power received at mobile k from the surrounding NodeBs:

$$I_k^{oth} = \sum_{y \in \mathcal{L} \setminus x} T_y \cdot d_{y,k} \quad (4)$$

We introduce now the boolean variable $\delta_{x,h}$ that indicates whether NodeB x serves at least one HSDPA user and is not in a ramping phase. Consequently, in case of the continuous scheme, $\delta_{x,h} = 1$ at all times. Furthermore, we follow [8] in defining the load of cell x with respect to cell y as

$$\eta_{x,y} = \sum_{k \in \mathcal{M}_x} \omega_{k,y} \quad (5)$$

with $\omega_{k,y} = \frac{\varepsilon_k^* \cdot R_k}{W} \cdot \begin{cases} \alpha & , \text{ if } \mathcal{L}(k) = y \\ \frac{d_{k,y}}{d_{k,\mathcal{L}(k)}} & , \text{ if } \mathcal{L}(k) \neq y. \end{cases}$

Using these variables we are able to formulate a compact equation of the total NodeB transmit power:

$$T_x = \delta_{x,h} \cdot T_x^* + (1 - \delta_{x,h}) \cdot \left(T_{x,c} + T_{x,r} + \sum_{y \in \mathcal{L}} \eta_{x,y} \cdot T_y \right) \quad (6)$$

where the DCH transmit power is given as

$$T_{x,d} = \sum_{y \in \mathcal{L}} \eta_{x,y} \cdot T_y. \quad (7)$$

Note that $T_{x,r} = 0$ if not in a ramping phase. In these equations, we neglected the thermal noise since it is by magnitudes smaller than the multiple access interference for a reasonable cell layout. The introduction of the vector

$$V[x] = \delta_{x,h} \cdot T_x^* + (1 - \delta_{x,h}) \cdot (T_{x,c} + T_{x,r}) \quad (8)$$

and the matrix

$$M[x,y] = (1 - \delta_{x,h}) \cdot \eta_{x,y} \quad (9)$$

leads to the following matrix equation

$$T = V + M \cdot T \Leftrightarrow T = (I - M)^{-1} \cdot V, \quad (10)$$

that is valid for all three power allocation schemes. The matrix I is the identity matrix, and T is the vector with the cell transmit powers T_x . The DCH and HSDPA transmit powers are then calculated with Eq. (7) and Eq. (1).

V. HSDPA BANDWIDTH MODEL AND TIME-DYNAMIC SIMULATION MODEL

In each TTI the scheduler in the NodeB decides on behalf of the CQI feedback which transport block size (TBS) and which user should be scheduled. The relation between SIR and CQI is given by the following formula [9]:

$$\text{CQI} = \max \left(0, \min \left(30, \left\lfloor \frac{\text{SIR}[\text{dB}]}{1.02} + 16.62 \right\rfloor \right) \right). \quad (11)$$

The instantaneous SIR at an HSDPA UE after combining in the RAKE receiver is the sum of the received signal powers of the propagation paths divided by the interference. Let us define $\Delta_T = \frac{T_{x,h}}{T_x}$ as the ratio between HS-DSCH transmit power and total transmit power. Then, the received SIR at a position f is

$$\gamma_f(\Delta_T) = \Delta_T \cdot \sum_{p \in \mathcal{P}_{x,f}} \frac{\xi_p}{\frac{I_f^{oth}}{T_x \cdot d_{x,f}} + \sum_{r \in \mathcal{P}_{x,f} \setminus p} \xi_r} \quad (12)$$

$$\text{with } I_f^{other} = \sum_{y \neq x} d_{y,f} \cdot T_y \cdot \sum_{r \in \mathcal{P}_{y,f}} \xi_r, \quad (13)$$

where ξ_p is an exponential random variable with mean β_p that describes the instantaneous propagation gain on path $p \in \mathcal{P}$. In this work, we assume the ITU Vehicular A model with 6 propagation paths. By inspection it can be stated that the influence of the other-cell interference on the SIR grows as the location is closer to the cell border. Hence, we model the mean and standard deviation of the SIR distribution at location f as a function of the other-to-own-interference-ratio $\Sigma_f = I_f^{oth}/(T_x \cdot d_{x,f})$ and introduce the *normalized* SIR $\Gamma_f = \gamma_f(1)$. By extensive simulations we have shown in [1] and in more detail in [10] that the dependency between Σ_f and mean and standard deviation of the normalized SIR distribution can be effectively approximated with a four-parametric Weibull function. Resulting from that, the location-dependent normalized SIR distribution is modeled in this work with an inverse Gaussian distribution. This leads directly to the distribution of the feedback CQI, $p_{\text{CQI},f}(q)$, which can be easily calculated by discretization of the normalized SIR distribution with (11). The mean TBS, i.e. the mean possible datarate at location f is then

$$E[\text{TBS}_f] = \sum_{q=0}^{30} p_{\text{CQI},f}(q) \cdot \min(\text{TBS}^*, \text{TBS}(q)), \quad (14)$$

where TBS^* is the maximum TBS that is possible with $N_{h,x}$ codes. The long-term bandwidth with round-robin scheduling, which we assume here, is then simply the mean value of the TBS corresponding to the CQI distribution, divided by the number of concurrently active HSDPA users:

$$R_f = \frac{1s}{N_h \cdot 2\text{ms TTI}} \cdot E[\text{TBS}_f] \quad (15)$$

Note that also MaxC/I scheduling or proportional scheduling can be modeled in a similar way by calculating additionally the probability that a user is scheduled.

Figure 2 shows a contour plot of the HSDPA long-term bandwidth versus Δ_T and Σ if 15 codes are available. It can be seen that the other-to-own interference ratio begins to influence

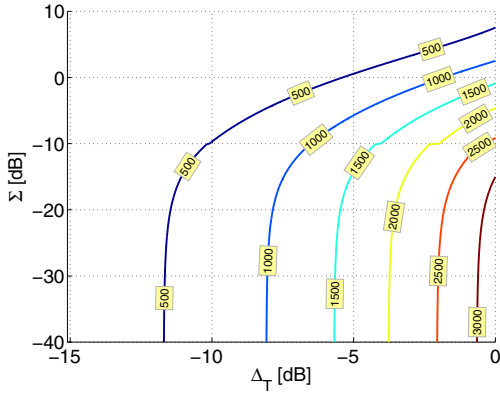


Fig. 2. Contour plot of the long term bandwidth for given Δ_T and Σ .

the bandwidth significantly with $\Sigma > -20$ dB. Note that the largest value for Δ_T is around -1 dB, which corresponds to a bandwidth of approx. 2800 kbps.

The long term bandwidth is now used in a time-dynamic simulation which considers the HSDPA data traffic of a user k as a flow with data volume V_k . The network area is discretized into a set of quadratic area elements. The time axis is divided in inter-event times, in which we assume that the users stay roughly within an area element. Events can be arrival events of DCH or HSDPA users, departure events, and POWER-UP and POWER-DOWN events. At the beginning of each inter-event time, for existing connections the DCH and HSDPA transmit powers are calculated according to the specific RRA scheme. If an arrival event occurs, additionally admission control for DCH and HSDPA is performed and the number of codes available for HSDPA are calculated according to the outcome of the admission control decision. Then, the bandwidth and the expected new departure times of each HSDPA user are calculated. At the end of an inter-event time, the remaining data volumes $V_{k,r}$ of the users are decreased by the data amount which has been transmitted within the current inter-event time.

In our simulation, we assume both DCH users and HSDPA flows arrive according to a Poisson process with arrival rate λ_s and λ_H , respectively. Dedicated channel users have an exponentially distributed call time with mean $E[T] = 120$ s, the HSDPA flow size is exponentially distributed with mean volume $E[V] = 100$ kbyte which is approximately the mean size of a web page. Note that thus the DCH connections follow a time-based user model, which means that the sojourn time of DCH connections is independent of the throughput, even if it would change during the lifetime of a connection. This is not the case for HSDPA-users, which stay into the system until they have transmitted their total data volume. This means that the lifetime of an HSDPA connection depends on the experienced throughput.

Admission control for the DCH connection is performed on base of the maximum allowed transmit power and on the available code resources on each new DCH arrival. For

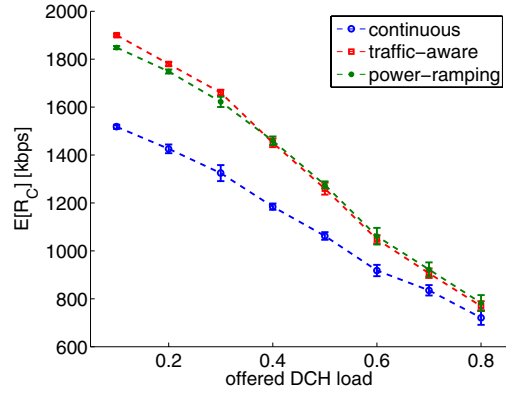


Fig. 3. Total HSDPA throughput vs. offered DCH load

this purpose, the required transmit power is calculated at the serving NodeB under assumption that all NodeBs send with maximum power in order to avoid outage. For the HSDPA we assume a count-based admission control which restricts the maximum number of concurrent connections to a fixed value.

VI. NUMERICAL RESULTS

For the numerical results the standard 19-cell network layout has been used, from which we only consider the middle cell. However, the complete network has been simulated such that the effect of the other-cell interference is properly captured. The distance between the NodeB antennas is 1.2 km. The maximum allowed transmit power per NodeB is 10 W, from which a constant share of $T_c = 2$ W is permanently reserved for the pilot and common channels. The arrival rate for the HSDPA flows is set to $\lambda_H = 1$ for all scenarios. The maximum number of HSDPA connections is 10.

In the first scenario, we increase the DCH offered load which is in this case defined with the occupied codes as

$$\rho_c = \frac{1}{C} \sum_{s \in S} \frac{\lambda_s}{\mu_s} \cdot c_s, \quad (16)$$

where c_s are the code requirements of service class s . We consider 128 kbps and 384 kbps users with a service mix of 0.6 to 0.4. With an increasing number of DCH users in the system, the resources available for the HS-DSCH decrease, which means that the HSDPA cell bit rate R_C also decreases. This is shown in Fig. 3. Notable is the large difference between the continuous on the one side and the traffic-aware and power-ramping scheme on the other side, which is around 250 kbps for lower DCH loads and is then diminishing with higher loads. The following reasons can be identified: first, the impact of other-cell interference. With the continuous scheme, the adjacent NodeBs send with full power even if no HSDPA user has to be served. The resulting additional interference decreases the mean SIR of the DCH and HSDPA users. This means that the DCH users require more transmit power in order to meet their target- E_b/N_0 -values, which increases the own-cell interference and decreases the transmit power

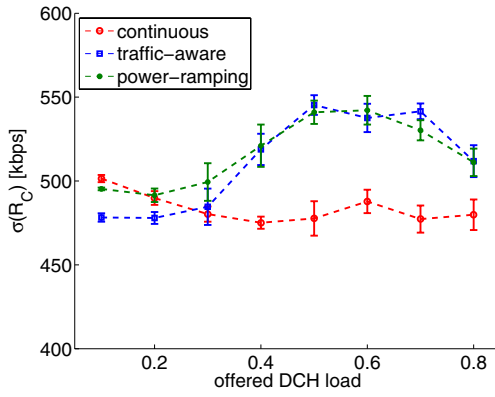


Fig. 4. Standard deviation of the HSDPA throughput vs. offered DCH load

available for the HSDPA. Additionally, the lower SIR due to other-cell interference lowers the HSDPA data rates directly. Secondly, since HSDPA user behavior follows a volume-based traffic model, higher bit rates mean also shorter sojourn times, which in turn leads to lower HS-DSCH activity and therefore again to lower interference in mean for the traffic-aware scheme. This phenomenon which leads to spatial heterogeneity even if the arrival process is spatially homogeneous is also described in [11] and [1].

Figure 4 shows the corresponding standard deviations of the cell throughput. With the continuous scheme the standard deviation is almost independent of the DCH load, while the influence of the varying other-cell interference in case of the traffic-aware and power-ramping schemes leads to a higher variability of the throughputs. Thus it can be concluded from this figure that the main factor on throughput variations is the ON-OFF pattern of interference due to that schemes. For high-load scenarios the throughput variation decreases again since in that case the system is in overload, meaning that the resources for HSDPA users are scarce. This leads to longer periods with switched on HS-DSCH since the users need longer to transmit their data volume, it is therefore again a side-effect of the volume-based user model.

The performance loss of the continuous scheme is also visible for the HSDPA blocking probabilities, as it can be seen in Fig. 5. Traffic-aware and power-ramping schemes lead to almost identical results, although it seems that the power-ramping schemes for higher DCH loads have slightly lower blocking probabilities than the traffic-aware scheme. An explanation for this behavior can be found by looking at the user throughput versus the distances, as shown in the next figure.

In Fig. 6, the conditional mean user throughput at a certain distance of the user to the NodeB for two scenarios with DCH loads 0.2 and 0.6 is shown. In case of a DCH load equal to 0.2, the continuous scheme leads to an almost constant performance loss of more than 200 kbps. The power-ramping scheme leads to slightly lower throughputs than the traffic-aware scheme due to the up-ramping at the beginning of a

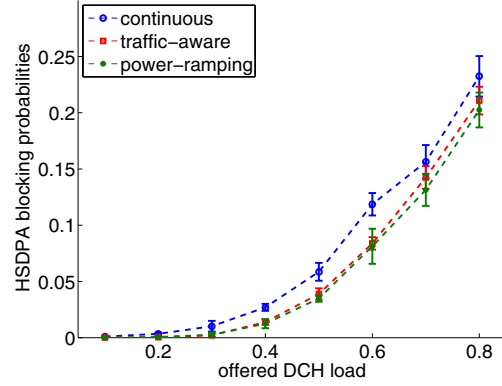


Fig. 5. HSDPA blocking probabilities vs. offered DCH load

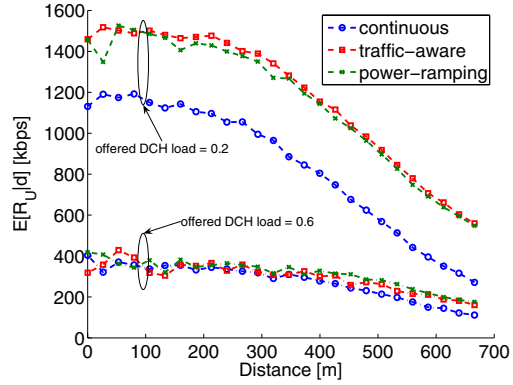


Fig. 6. Mean user throughput vs. distance

HSDPA transmission. However, in case of a DCH load of 0.6, the power-ramping scheme shows better results than the traffic-aware scheme for larger distances, which is counter-intuitive at first sight. An explanation for this behavior is that DCH users in surrounding cells generate more other-cell interference the higher the transmit power in the “own” cell is, which leads in turn to lower bit rates for HSDPA users close to the cell border. Since this dependency is non-linear, the power-ramping scheme causes less other-cell interference such that especially users at the cell border can profit. In case of the traffic-aware scheme, the transmission with maximum power leads therefore effectively to lower bit rates for users close at the cell border. Which is also interesting is the fact that the performance loss for the continuous scheme is nearly independent of the distance, although the additional interference is higher for users which are closer to the cell edge. The reason for this behavior may be the employed round-robin scheduling, which distributes the resources time-fair between all users. This means that if users stay longer in the system on the cell edges, they also affect users in the inner area by taking away resources.

Figure 7 shows the CDF of the DCH transmit powers. It can be seen that for higher DCH loads, the power-ramping scheme requires slightly less DCH transmit power, so it supports the observation we made for the conditional throughput in Fig. 6.

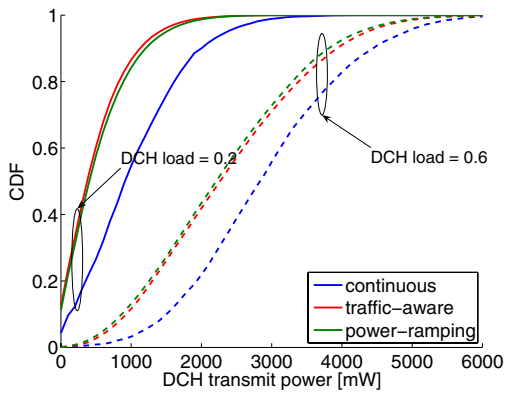


Fig. 7. CDF of DCH transmit powers

Note that although the impact of this effect is quite small it is also visible in Fig. 3 and Fig. 5. This figure also shows the large impact of the HS-DSCH transmit power on the power requirements of the DCH users. The increase between the cases with a DCH-load of 0.2 and 0.6 is mostly due to the additional interference by DCH users, however with a load of 0.2 the benefit for the DCH users with traffic-aware and power-ramping scheme is higher than in the case with a load of 0.6, as it can be seen on the steeper curve progressions in the first case.

Finally, we compare in Fig. 8 the distribution of the user throughput for a DCH load of 0.2 for the inner and outer area of the middle cell, which is distinguished for regions with high and low own-to-other-cell interference ratio. As expected in the outer region, the throughput is generally lower than in the inner of the cell, and the continuous scheme has in both cases lower throughputs. The maximum throughput in the inner cell area is with the chosen multipath propagation profile around 2700 kbps, where in the outer area the maximum throughput is around 2000 kbps. The stair-like shape of the curves for the inner cell are due to the number of concurrent users in the system: At 1500 kbps and higher, only one user is in the system, beginning from 900 kbps two users, and so on.

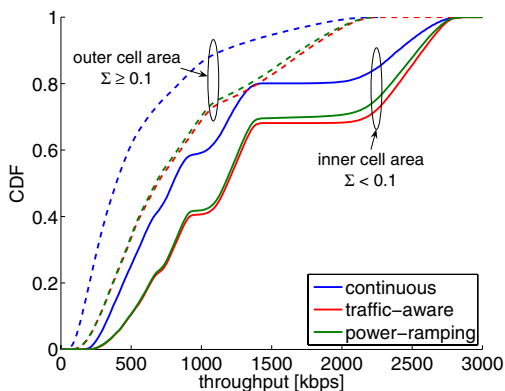


Fig. 8. CDF of user throughput for inner and outer cell area

VII. CONCLUSION

In this paper we investigated different power allocation schemes for the HSDPA with help of a flow-based simulation which includes DCH and HSDPA users. The simulation models the complete interference situation in the network and implements an HSDPA long-term bandwidth model which considers the distribution of the received signal-to-noise ratio depending on the user location. We showed that the additional interference caused by the continuous power allocation scheme leads to significant performance losses for the HSDPA users. The power-ramping scheme shows almost equal results to the traffic-aware scheme with instant on-off switching of the HS-DSCH. Additionally, if more DCH users are in the system, the power-ramping scheme shows slightly better results than the traffic-aware scheme, which is a phenomenon which could be investigated in more detail in future work. Further aspects would be a detailed simulation with the inclusion of slot-wise power control commands, more heterogeneous networks and other scheduling disciplines, as well as a sensitivity analysis regarding the flow-size distribution.

REFERENCES

- [1] A. Mäder, D. Staehle, and H. Barth, "A Novel Performance Model for the HSDPA with Adaptive Resource Allocation," in *Proc. of the 20th ITC*, ser. LNCS, L. Mason, T. Drwiega, and J. Yan, Eds., vol. 4516. Ottawa, Canada: Springer, June 2007, pp. 950–961.
- [2] A. Mäder and D. Staehle, "Impact of HSDPA Radio Resource Allocation Schemes on the System Performance of UMTS Networks," in *Proc. of IEEE VTC Fall '07*, Baltimore, MD, USA, Sept. 2007.
- [3] K. I. Pedersen, *et al.*, "Network Performance of Mixed Traffic on High Speed Downlink Packet Access and Dedicated Channels in WCDMA," in *Proc. of IEEE VTC Fall '04*, Milan, Italy, Sept. 2004, pp. 2296–4500.
- [4] K. Hiltunen, M. Lundevall, and S. Magnusson, "Performance of Link Admission Control in a WCDMA System with HS-DSCH and Mixed Services," in *Proc. of PIMRC '04*, Barcelona, Spain, Sept. 2004.
- [5] 3GPP, "3GPP TS 25.321 V6.6.0 Medium Access Control (MAC) protocol specification," 3GPP, Tech. Rep., Sept. 2005.
- [6] D. Staehle, "On the Code and Soft Capacity of the UMTS FDD Downlink and the Capacity Increase by using a Secondary Scrambling Code," in *IEEE PIMRC '05*, Berlin, Germany, Sept. 2005.
- [7] H. Holma and A. T. (Eds.), *WCDMA for UMTS*. John Wiley & Sons, Ltd., Feb. 2001.
- [8] D. Staehle and A. Mäder, "An Analytic Model for Deriving the Node-B Transmit Power in Heterogeneous UMTS Networks," in *IEEE VTC Spring '04*, Milano, Italy, 2004.
- [9] F. Brouwer, *et al.*, "Usage of Link-Level Performance Indicators for HSDPA Network-Level Simulations in E-UMTS," in *Proc. of IEEE ISSSTA '04*, Sidney, Australia, Aug. 2004, pp. 844–848.
- [10] D. Staehle and A. Mäder, "A Model for Time-Efficient HSDPA Simulations," in *Proc. of IEEE VTC Fall '07*, Baltimore, MD, USA, Oct. 2007.
- [11] R. Litjens, J. van den Berg, and M. Fleuren, "Spatial Traffic Heterogeneity in HSDPA Networks and its Impact on Network Planning," in *Proc. of ITC 19*, Beijing, China, Aug. 2005, pp. 653–666.